Flow dynamics at the minimum starting condition of a supersonic diffuser to simulate a rocket's high altitude performance on the ground [†]

Hyo-Won Yeom, Sangkyu Yoon, Hong-Gye Sung[*]

School of Aerospace and Mechanical Engineering, Korea Aerospace University
2001-1 Hwajeon-Dong, Deogyang-Gu, Goyang-City, Gyeonggi, 412-791, South Korea

---

Abstract

A numerical analysis was conducted to investigate and characterize the unsteadiness of the flow structure and oscillatory vacuum pressure inside of a supersonic diffuser equipped to simulate high-altitude rocket performance on the ground. A physical model including a rocket motor, vacuum chamber, and diffuser, which have axisymmetric configurations was employed. Emphasis was placed on investigating the physical phenomena of very complex and oscillatory flow evolutions in the diffuser operating very close to the starting condition, i.e. at a minimum starting condition, which is one of the major important parameters from a diffuser design point of view.

Keywords: Compressible turbulent flow; High altitude test facility; Minimum starting condition; Shock train; Supersonic diffuser

---

1. Introduction

A rocket motor designed to operate at high altitudes needs a nozzle with a large expansion ratio in order to maximize thrust at much lower atmospheric pressures than that at sea level. When these motors are tested on the ground, accurate performance cannot be proven due to flow separation occurring in the nozzle. Therefore, to accurately evaluate the performance of such rocket motors, a high altitude test facility system is required to test the rocket motor at high altitude conditions on the ground. One such system is the supersonic exhaust diffuser, and another is an ejector to simulate high altitude conditions on the ground. The simplest method among these is to use a supersonic exhaust diffuser.

Studies on testing methods, design methods, and the internal flow of experimental systems simulating

---

high altitude conditions have been performed in research institutes, industries, and academic labs since the mid-1950s. In the US, experiments and theoretical analyses on various performance factors were performed at the government sponsored AEDC (Arnold Engineering Development Center) in order to research and develop ground experimental equipment that can simulate high altitude conditions [1-3]. In brief, the AEDC proposed theoretical methods to determine the starting pressure of various types of diffusers (long cylindrical diffusers, long second throat diffusers, short second throat diffusers, etc.) [1-4]. In India, experiments using both cold nitrogen gas and hot rocket exhaust gas as driving fluids were carried out at the ISRO (Indian Space Research Organization) to design a high altitude test (HAT) facility that can be used to test the third stage motor (Ps-3) of a Polar Satellite Launch Vehicle [8]. In France, the DGA/CAEPE developed the high altitude test facility MESA, which consists of a vacuum pump, ejector, and diffuser. Further, four diffuser experiments were performed at the ONERA R1Ch facility in order to find an optimum configuration by way of a numerical

analysis used to evaluate experimental data collected at the facility [9]. In the most recent research, Purdue University developed a lab-scale high altitude facility in order to supply a hybrid rocket motor with an air-powered ejector and blow-off door for the initial lower back pressure [10].

For two decades, numerical investigations were conducted in order to understand internal shock structures and flow physics in the supersonic ejector/diffuser system [11-14]. These numerical studies have focused on flow structure at steady state with week considerations of compressible turbulent effects. As the Mach number of a turbulent flow increases, the velocity fields can no longer be assumed to be solenoidal. Turbulent modeling for compressible flow has to account for the additional correlations involving both the fluctuating thermodynamic quantities and the fluctuating dilatation. The interaction of a shock wave with a turbulent boundary layer leads to a significant increase in turbulence intensity and shear stress across the shock [16]. To take account of the important feature at high-speed flow, in this study, a combined model of the low Reynolds number k-ε model [15] and compressible-dissipation and pressure-dilatation proposed by Sarkar [16-18] was proposed. And also unsteady numerical analysis was performed in order to consider unsteadiness of the flow structure and oscillatory vacuum chamber pressure at minimum start-operating condition.

For this paper, a numerical simulation was conducted in order to comprehend the detailed flow evolution information in the diffuser operating at a minimum starting condition, which is blinded in experiments, but is very important from a diffuser design point of view. The minimum starting pressure is one of the major factors required to determine the size of the test facility such as the driving fluid supply system, rocket and diffuser sizes, and so on.

2. Numerical method

2.1 Governing equation

The Favre averaged governing equations based on the conservation of mass, momentum, and energy for a compressible, chemically reacting gas can be written as

$$\frac{\partial \bar{\rho}}{\partial t} + \frac{\partial \bar{\rho}\tilde{u}_j}{\partial x_j} = 0 \quad (1)$$

$$\frac{\partial \bar{\rho}\tilde{u}_i}{\partial t} + \frac{\partial \left(\bar{\rho}\tilde{u}_i\tilde{u}_j + \bar{p}\delta_{ij} \right)}{\partial x_j} = \frac{\partial \left(\bar{\tau}_{ij} - \overline{\rho u_j'' u_i''} \right)}{\partial x_j} \quad (2)$$

$$\frac{\partial \bar{\rho}\tilde{E}}{\partial t} + \frac{\partial \left(\left(\bar{\rho}\tilde{E} + \bar{p} \right)\tilde{u}_j \right)}{\partial x_j} = \frac{\partial \left(\tilde{u}_i\bar{\tau}_{ij} - \overline{\rho h'' u_i''} \right)}{\partial x_j} - \frac{\partial \bar{q}_j}{\partial x_j} \quad (3)$$

2.2 Turbulence closure

The standard k-ε model, which was proposed for high Reynolds number flows, is traditionally used with a wall function and the variable y^+ as a damping function. However, universal wall functions do not exist in complex flows, and the damping factor cannot be applied to flows with separation. Thus, a low Reynolds number k-ε model was developed for near-wall turbulence. Within certain distances from the wall, all energetic large eddies will reduce to Kolmogorov eddies (i.e. the smallest eddies in turbulence), and all the important wall parameters, such as friction velocity, viscous length scale, and mean strain rate at the wall can be characterized by the Kolmogorov micro scale.

Yang and Shih [15] proposed a time-scale-based k-ε model for the near-wall turbulence related to the Kolmogorov time scale as its lower bound so that the equation can be integrated to the wall. The advantages of this model are (a) no singularity at the wall, and (b) adaptability to separation flow since the damping function is based on the Reynolds number instead of y^+. Low Reynolds number models have been designed to maintain the high Re formulation in the log-law region and further tuned to fit measurements for the viscous and buffer layers.

The turbulent kinetic energy and its dissipation rate are calculated from the turbulence transport equations written in the following:

$$\frac{\partial \bar{\rho}\tilde{k}}{\partial t} + \frac{\partial \left(\bar{\rho}\tilde{u}_j\tilde{k} \right)}{\partial x_j} = \frac{\partial}{\partial x_j}\left(\left(\mu + \frac{\mu_t}{\sigma_k} \right)\frac{\partial \tilde{k}}{\partial x} \right) + P_k - \bar{\rho}\tilde{\varepsilon} \quad (4)$$

$$\frac{\partial \bar{\rho}\tilde{\varepsilon}}{\partial t} + \frac{\partial \left(\bar{\rho}\tilde{u}_j\tilde{\varepsilon} \right)}{\partial x_j} = \frac{\partial}{\partial x_j}\left(\left(\mu + \frac{\mu_t}{\sigma_\varepsilon} \right)\frac{\partial \tilde{\varepsilon}}{\partial x} \right) + \frac{\left(C_{\varepsilon 1}P_k - C_{\varepsilon 2}\bar{\rho}\tilde{\varepsilon} \right)}{T_t} + \Lambda \quad (5)$$

where P_k, T_t and Λ are turbulent kinetic energy production rate, turbulent time scale, and damping function, respectively, and then represented as follows:

$$P_k = \left(\mu_t \left(\frac{\partial \tilde{u}_i}{\partial x_j} + \frac{\partial \tilde{u}_j}{\partial x_i} - \frac{2}{3} \frac{\partial \tilde{u}_k}{\partial x_k} \delta_{ij} \right) - \frac{2}{3} \bar{\rho} \tilde{k} \delta_{ij} \right) \frac{\partial \tilde{u}_i}{\partial x_j} \qquad (6)$$

$$T_t = \frac{\tilde{k}}{\tilde{\varepsilon}} + \tau_k \qquad (7)$$

$$\tau_k = C_k \left(\frac{\nu}{\varepsilon} \right)^{1/2} \tau_k \qquad (8)$$

$$\Lambda = \nu \mu_t \left(\frac{\partial \tilde{u}_i}{\partial x_j \partial x_k} \right)^2 \qquad (9)$$

where τ_k is the Kolmogorov time scale.

The turbulent viscosity and damping factor f_μ for the wall effect can be written as

$$\mu_t = \bar{\rho} C_\mu f_\mu \tilde{k} T_t \qquad (10)$$

$$f_\mu = \left[1 - exp\left(-a_1 R_y - a_3 R_y{}^3 - a_5 R_y{}^5 \right) \right]^{1/2} \qquad (11)$$

The damping factor is taken to be a function of $R_y = k^{1/2} y / \nu$.

The following constants are used.

$\sigma_k = 1.0$, $\sigma_\varepsilon = 1.3$, $C_\mu = 0.09$, $C_{\varepsilon 1} = 1.44$,
$C_{\varepsilon 2} = 1.92$, $a_1 = 1.5 \times 10^{-4}$, $a_3 = 5.0 \times 10^{-7}$,
$a_5 = 1.0 \times 10^{-10}$

The low Reynolds number model used in this work is based on the combined model of Yang and Shih and Sarkar's compressed model [16-18].

2.3 Numerical scheme

The conservation equations for moderate and high Mach number flows are well coupled, and standard numerical techniques perform adequately. In regions of low Mach number flows, however, the energy and momentum equations are practically decoupled and the system of conservation equations becomes stiff. In the entire diffuser system, the flow fields are governed by a wide variety of time scales (from supersonic flow of the rocket jet to stagnation-flow in the vacuum chamber). Such a wide range of time scales causes an unacceptable convergence problem. Indeed, the author experienced that the conventional numerical scheme could not calculate the vacuum chamber pressure accurately. To overcome the problem, a dual time-integration procedure designed for all Mach number flows is applied, which may be constructed in two steps. First, a rescaled pressure term is used in the momentum equation to circumvent the singular behavior of pressure at low Mach numbers. Second, a dual time-stepping integration procedure is established.

The pseudo-time derivative may be chosen to optimize the convergence of the inner iterations by using an appropriate preconditioning matrix that is tuned to rescale the eigenvalues to render the same order of magnitude to maximize convergence. To unify the conserved flux variables, a pseudo-time derivative of the form $\Gamma \partial Z / \partial \tau$ can be added to the conservation equation. Since the pseudo-time derivative term disappears upon convergence, a certain amount of liberty exists in choosing the variable Z. We took advantage of this by introducing a pressure p' as the pseudo-time derivative term in the continuity equation.

While dual time stepping and LU-SGS are applied for time integration, a control volume method is used to integrate both inviscid fluxes represented by AUSMPW+ and MUSCL and viscous fluxes represented by central difference. The code is paralleled with a multi-block feature by using an MPI library to speed up the unsteady calculation.

3. Results and discussion

Previous work shows that 1) an increase in the compressibility level tends to increase the decay rate of turbulent kinetic energy, k, and 2) the direct numerical simulation results present that moderate compressibility affects compressible dissipation and no solenoidal dissipation [16]. For this study, the author determined that the low Reynolds number k-ε model with Sarkar's compressed model provided good agreement with the experimental data after testing several other two-equation turbulent models, which will be prepared for another research paper.

3.1 Diffuser configurations

A test model with a large vacuum chamber is illustrated in Fig. 1. The physical sizes of the test models were decided upon in order to investigate the effect that major design parameters such as the area ratio of the diffuser to the rocket nozzle throat (A_d / A_t), the expansion ratio of the rocket nozzle (A_e / A_t), and the rocket nozzle throat diameter to start the diffuser.

The dimensions of the model are diffuser length L of 260mm, diffuser diameter D of 21 mm, the ratio of length to diameter of diffuser L/D of 12.38, the area ratio of diffuser to rocket motor nozzle throat A_d / A_t of 56.25, and the area ratio of diffuser exit to rocket motor nozzle throat A_e / A_t of 35.02 (Fig. 1). Experiments using cold nitrogen gas ($\gamma = 1.4$) as a driving fluid were carried out.

Fig. 2 shows the computational domain concerned in this study. The computational configuration is exactly the same as that of the experiment except the vacuum chamber configuration, but with the same volume size so as to not lose any accuracy and promote the numerical convergence rate. The computation domain consisted of three blocks, and each block grid was 115*50, 79*30, and 206*79, respectively. The wall conditions on the front of vacuum chamber as well as the stagnation pressure and temperature in the rocket chamber were applied, respectively. The wall was assumed to be an adiabatic wall, while partially subsonic and supersonic conditions depending on the flow condition were applied for the exit of the diffuser. A total of eight processors participated for parallel computation.

3.2 Diffuser operation characteristics

The starting process of the supersonic exhaust diffuser can be explained through Fig. 3 in Ref. [3]. In region (1), both the nozzle and diffuser are un-started. The jet momentum exhausted from the rocket is not sufficient for the flow to fulfill the nozzle, so the flow is separate from the nozzle wall. However, as P_o / P_a increases further, the nozzle flows full but over-expands, so the diffuser is still un-started in region (2). The un-started regime consists of two phases. In the first phase, the flow separates from the nozzle wall through oblique shock, and in the second phase, the flow separation occurs at the nozzle exit. As P_o / P_a increases further to $(P_o / P_a)_{st,min}$, the diffuser also flows full so that the shock system is fully established in the duct. In this regime, the under-expanded supersonic jet from the nozzle impinges on the diffuser wall. At this stage, the supersonic exhaust diffuser is said to have started, and the corresponding pressure ratio is the minimum starting pressure ratio $(P_o / P_a)_{st,min}$.

In this study, all three of the above operation regimes are simulated for the case of the area ratio of the diffuser cross section to the nozzle throat $A_d / A_t = 56.25$ in order to observe the flow structure and validate the numerical results. At 10 bar of the rocket chamber, the diffuser operation regime belongs to region (1) in Fig. 3. The flow separates inside the nozzle so that the exhaust jet cannot impinge on the diffuser wall as shown in Fig. 4(a).

Because the flow in the diffuser belongs to the subsonic regime, pressure along the wall increases gradually to the same level as atmospheric pressure from
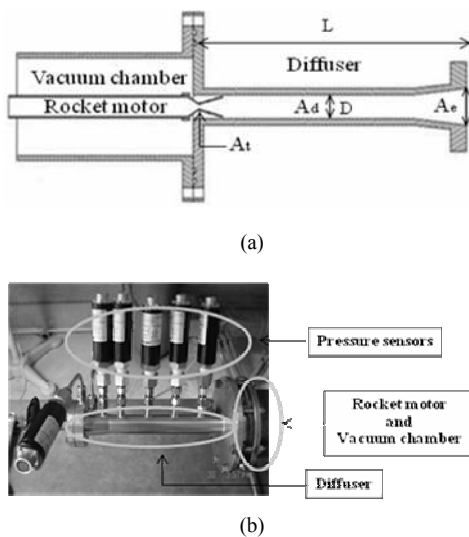

(a)

(b)

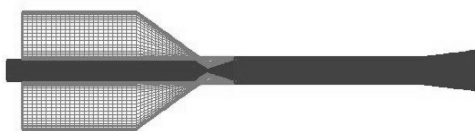Fig. 1. Schematics (a) and photo (b) of a model diffuser Ref. [19].

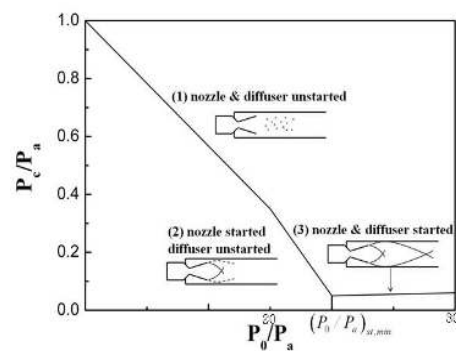Fig. 2. Computational domain consisting of three blocks.

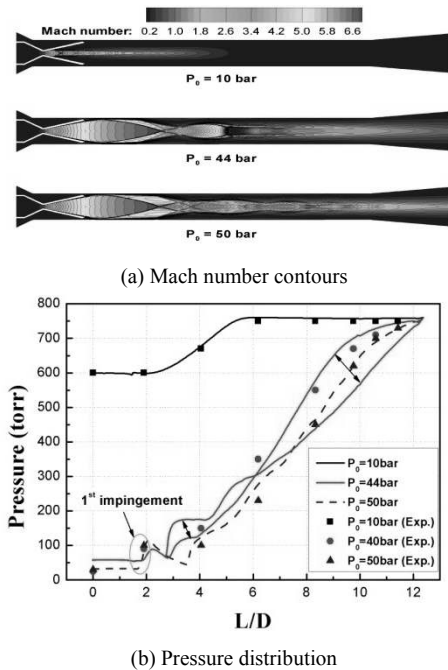Fig. 3. Typical diffuser characteristic curve of Ref. [3].

(a) Mach number contours

(b) Pressure distribution

Fig. 4. Mach number contours and pressure distribution along the diffuser wall with $A_d / A_t = 56.25$.

the somewhat low pressure in the vacuum chamber due to the suction of the inside flow of the vacuum chamber into the jet boundary, as shown in Fig. 4(b). Experimental values are marked as symbols and numerical values are represented as lines. Both values are in fairly good agreement. Since the mass flux of the jet at 10 bar is not sufficient to start the diffuser, the rocket chamber pressure increases to 44 bar, roughly the starting pressure of the diffuser. The experimental deviation of operation pressure at 40 bar may be about 4 bar [19]. Numerical data at 44 bar more properly simulated dynamic motion of shock train in the diffuser. The numerical comparison at 40 bar and 44 bar is more precisely described in the next section. And then the jet exhausting from the rocket nozzle impinges on the diffuser wall as shown in Fig. 4(a). The pressure in the vacuum chamber is evacuated to around 50 torr from 1 bar, proving that the diffuser is working. The pressure rises behind the impinging point of the jet on the diffuser wall, decreases in the expansion region, increases again during the next compression wave, and then finally rises to atmospheric pressure at the exit of the diffuser. The experimental data and the numerical results appear to reveal a discrepancy, but the unsteady flow motions in the diffuser are blinked on the background of the
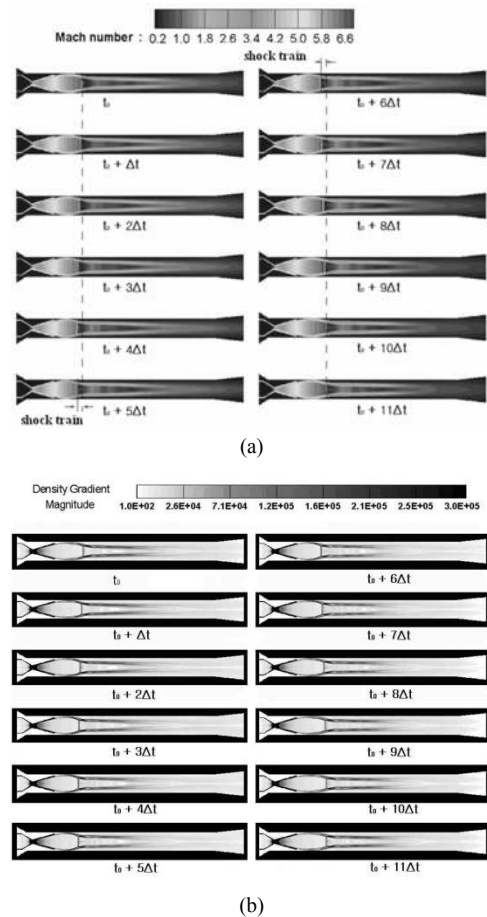

(a)

(b)

Fig. 5. Flow evolution in a diffuser at motor pressure 40 bar with $A_d / A_t = 56.25$ ($\Delta t = 0.1$ msec): (a) Mach number contours, and (b) shadowgraph..

instantaneous data, which is described in detail in the next section. If the motor pressure increases further, the jet strength impinging on the diffuser wall also increases as expected. The motor pressure of 50 bar provides two peaks of pressure along the diffuser due to two impingements on the diffuser wall. The numerical results compare fairly well with the experimental data, in a different view as shown at 44 bar of the rocket motor. Insights from a detailed comparison reveal that a dynamic analysis on both the numerical and experimental tasks is essential in order to avoid a misleading or incomplete conclusion based on the static analysis.

3.3 Flow dynamics in a diffuser

As described in section 3.2, the flow structures in the diffuser are classified according to three operation
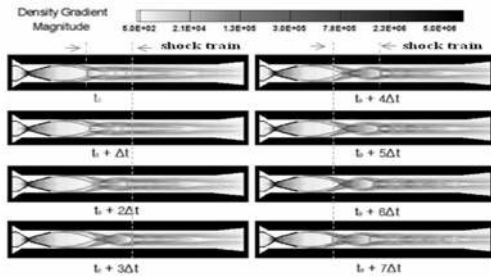
Fig. 6. Flow evolution in a diffuser at motor pressure 44 bar with $A_d / A_t = 56.25$ ($\Delta t = 0.1$ msec).

(a)

(b)

Fig. 7. Pressure distribution in the diffuser both along the wall and at centerline at motor pressure 40 bar and 44 bar with $A_d / A_t = 56.25$.

regimes of a diffuser from a global view points. In this study, detailed flow structures at the diffuser starting point are accurately examined for two reasons: 1) minimum starting pressure is a very important design parameter of a diffuser because the starting pressure affects the size of the test facilities, and 2) a steady calculation to investigate the flow structure and to predict pressure value in a diffuser may lead to an incorrect decision because the exact experiments to determine the minimum starting pressure of a diffuser are very critical.

Fig. 5 shows the flow evolution of the Mach number and numerical shadow graph at 40 bar. The normal shock moves back and forth from a reference position with a 0.8 msec periodic time. The acoustic waves traveling inside of the diffuser may induce a shock train.

If the rocket pressure increases to 44 bar, the shock train structure shows different features (Fig. 6).

A small supersonic pocket behind the first diamond shock occurred at the axis of the diffuser and periodically moved down- and up-stream. The period of oscillation relates to the acoustic mode in the subsonic region after the first diamond shock. The length of the shock is further away from the reference position than that of 40 bar. The following physical phenomena may provide an explanation: 1) the mass flux at 44 bar is sufficient to produce the second shock pocket but not as strong as the first diamond shock, and 2) the coupling of acoustic waves and flow evolution can easily excite the movement of the second shock pocket.

Even though the rocket pressure remains constant as 40 or 44 bar, the flow structure shows different features as described above. While only one shock pocket is generated at 40 bar, two shock pockets are generated at 44 bar. Since only one shock occurs at 40 bar and the pressure traveling from downstream to
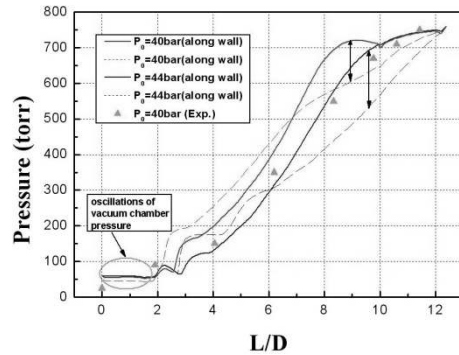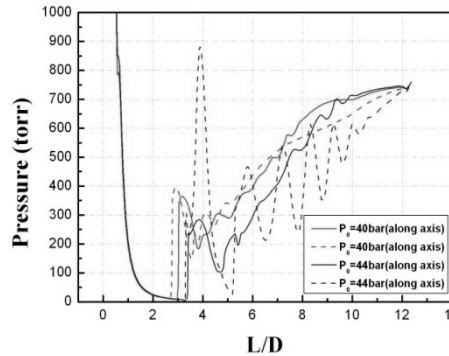
upstream penetrates into the vacuum chamber so it provides pressure fluctuations in the vacuum chamber, as shown in Fig. 7 (a). However, at 44 bar, the pressure wave traveling from downstream to upstream cannot penetrate the first shock pocket, so the pressure change at the vacuum chamber is negligible, as shown in Fig. 7 (a): one line of 44 bar splits into two lines after the first impingement position of the shock at a different time frame, but the pressure still fluctuates slightly because the pressure information can transfer into the vacuum chamber through a boundary layer even though its strength is greatly attenuated. Figure 8 shows the shadowgraphs zoomed into near the shock impingement for the two cases. At 40 bar, the boundary length of the impingement and supersonic area are much shorter than those of 44 bar, which proves the above claim. Fig. 7 (b) shows the pressure along the axis. The first normal shock position at 40 bar is further upstream, but the amplitude of the fluctuation provides a much higher value at 44 bar, revealing that the coupling between acoustic wave

Shock impingement

(a)
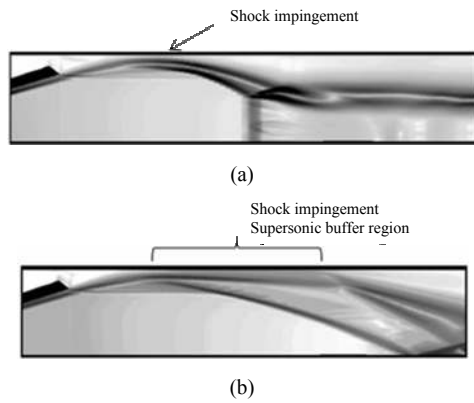
Shock impingement
Supersonic buffer region

(b)

Fig. 8. Numerical shadowgraphs near shock impingement on the diffuser at motor pressure (a) 40 bar and (b) 44 bar with $A_d / A_t = 56.25$.

and flow evolution may produce over-pressurization and thus induce over-oscillation of the test facility structure if those frequencies match exactly.

4. Conclusion

The unsteadiness of a flow structure and pressure inside a supersonic diffuser for simulating a rocket's high altitude environment on the ground was numerically investigated by treating the conservation equations of mass, momentum, and energy. The present model takes into account a compressible low-Reynolds-number k-ε turbulent model.

The computational geometry consists of the entire diffuser flow path from the rocket chamber and vacuum chamber in stagnation conditions to the exhaust of the diffuser. While dual time stepping and LU-SGS were applied for time integration, the control volume method was used to integrate inviscid fluxes represented by AUSMPW+ and MUSCL as well as viscous fluxes by central difference. Eight processors participated for parallel computation by using an MPI library.

Unsteady numerical calculations were quite comparable to the experimental data and convey valuable information to investigate unsteadiness of the diffuser's operation, especially at a rocket chamber pressure close to the minimum starting condition of the diffuser. At 10 bar (the un-start condition) and 50 bar (a much higher pressure than the starting pressure) the pressures along the diffuser wall show relatively steady data. If the diffuser starts, the vacuum chamber pressure has a typical value of about 50 torr, which belongs to an atmospheric pressure of around 20-25

km altitude. The vacuum pressure remained constant even though higher rocket chamber pressure than that at the starting condition was supplied. At the minimum starting pressure (40 bar), both the vacuum chamber pressure and the wall pressure periodically oscillated due to the shock train. However, somewhat above the starting pressure at 44 bar, the pressure along the center line showed much greater amplitudes than that for the case of 40 bar, but the vacuum chamber pressure negligibly oscillated due to the much larger size of the boundary length of the shock impingement and supersonic area that attenuates pressure oscillation transferring through the boundary layer. This information may be very valuable to determine the minimum operating pressure of the diffuser from economic and stable diffuser-design points of view.

References

[1] J. N. Sivo, C. L. Meyer and D. J. Peters, Experimental Evaluation of Rocket Exhaust Diffusers for Altitude Simulation, *NASA-TN-D-298*, 1960.

[2] B. H. Goethert, High Altitude and Space Simulation Testing, *ARS Journal*, 1962, pp872-882.

[3] P. F. Massier and E. J. Roschke, Experimental Investigation of Exhaust Diffusers for Rocket Engines, *JPL-TR-32-210*, 1962.

[4] R. C. German, R. C. Bauer and J. H. Panesci, Methods for Determining the Performance of Ejector-Diffuser Systems, *Journal of Spacecraft and Rockets*, 3 (2) (1966) 193-200.

[5] C. J. Wojciechowski and P. G. Anderson, Parametric Analysis of Diffuser Requirements for High Expansion Ratio Space Engine, LMSC-HREC-TR-D784489, *NASA-CR-161924*, 1981.

[6] R. McAmis and C. Bartlett, Aerodynamic Free-Jet Nozzle Performance Augmentation Using An Exhaust Diffuser, *AIAA* Paper 91-2270, 27th *AIAA/ASME/SAE/ASEE Joint Propulsion Conference & Exhibit*, Sacramento, CA, 1991.

[7] S. E. Stephens, Experimental and Computational Data from a Small Rocket Exhaust Diffuser, *AIAA*

Paper 93-1860, *29th AIAA/ASME/SAE/ASEE Joint Propulsion Conference & Exhibit,* Monterey, CA, 1993.

[8] K. Annamalai, K. Visvanathan, V. Sriramulu and K. A. Bhaskaran, Evaluation of the performance of supersonic exhaust diffuser using scaled down models, *Experimental Thermal and Fluid Science*, Vol. 17, Issue 3, July, 1998, pp. 217-229.

[9] L. Quebert and Y. Garcia, Theoretical and Experimental Design of an Exhaust Diffuser for an Upper Stage Engine of a Ballistic Missile, *AIAA* Paper 2001-3382, *37th AIAA/ASME/SAE/ASEE Joint Propulsion Conference & Exhibit*, Salt Lake City, Utah, 2001.

[10] M. R. Otterstatter, S. E. Meyer, S. D. Heister, E. M. Dambach, Design of an Altitude-testing Facility for Lab-Scale Propulsion Devices, *AIAA* Paper 2007-5323, 43rd *AIAA/ASME/SAE/ASEE Joint Propulsion Conference & Exhibit*, Cincinnati, OH, 2007.

[11] S. Sankaran, T. N. V. Satyanarayana, K. Annamalai, K. Visvanathan, V. Babu and T. Sundararajan, "CFD Analysis for Simulated Altitude Testing of Rocket Motors," *Canadian Aeronautics and Space Journal*, Vol. 48, No. 2, 2002, pp. 153-162.

[12] Falin Chen, C. F. Liu and J. Y. Yang, "Supersonic Flow in the Second-Throat Ejector-Diffuser System," *Journal of Spacecraft and Rockets*, 31 (1) (1994) 123-129.

[13] Y. Bartosiewicz, Zine Aidoun, P. Desevaux and Yves Mercadier, "Numerical and Experimental Investigations on Supersonic ejectors," *International Journal of Heat and Fluid Flow*, 26, 2005, pp. 56-70.

[14] Kazuyasu Matsuo, Yoshiaki Miyazato and Heuy-Dong Kim, "Shock train and Pseudo-shock Phenomena in Internal Gas Flows," *Progress in Aerospace Sciences*, 35, 1999, pp. 33-100.

[15] Z. Yang and T. H. Shih, New Time Scale Based Model for Near-Wall Turbulence, *AIAA Journal*, 31 (7) (1993) 1191-1197.

[16] S. Sarkar, B. Erlebacher, M. Hussaini and H. Kreiss, "The Analysis and Modeling of Dilational Terms in compressible Turbulence." *Journal of Fluid Mechanics*, 227 (1991) 473-493.

[17] S. Sarkar, "Modeling the Pressure-Dilatation Correlation," *ICASE*, Rept. 91-42, Hampton, VA, May 1991.

[18] S. Dash and D. C. Kenzakowski, "A Compressible-dissipation extension of the k-epsilon Turbulence Model and Building-Block data for its Validation," AIAA-1992-2766, *AIAA and SDIO*, *Annual Interceptor Technology Conference*, Huntsville, AL, May 19-21, 1992. 28 p.

[19] Y. Kim, "Experimental Study on a Design of Diffuser for Simulating High-Altitude Environment," Annual Report, Korea Aerospace Research Institute, 2007.R. S. Chandel and S. R. Bala, Effect of welding parameters and groove angle on the soundness of root beads deposited by the SAW process, *Proc. of Trends in Welding Research*, Gatlinburg, Tennessee, USA (1986) 479-385.

Hyo-Won Yeom received a B.S. degree in the department of Aerospace & Mechanical Engineering from Korea Aerospace University in 2007. He is currently a master candidate at the school of Aerospace & Mechanical Engi-neering at Korea Aerospace Uni-versity in Goyang-city, Korea. His research interests are in the area of numerical analysis for High-speed propulsion system.

Sangkyu Yoon received a B.S. degree in the department of Aerospace & Mechanical Engineering from Korea Aerospace University in 2006 and M.S. degrees in the school of Aerospace & Mecha-nical Engineering from Korea Aerospace University in 2008. He currently works in Hanwha Corporation R&D Center.

Hong-Gye Sung received a B.S. degree in the department of Aerospace Engineering from Inha University in 1984 and Ph.D. degree in Nuclear and Mechanical Engineering from The Pennsylvania State University in 1999. Dr. Sung has various research experiences in the fields of high-speed propulsion and rocket propulsion in Agency for Defense Development for 22 years (1984-2006). He is currently a professor at the School of Aerospace and Mechanical Engineering of Korea Aerospace University in Goyang, Korea. Dr. Sung's research interests are in the area of propulsion, combustion, and its control.